A Transient Fault-signal Extraction Scheme for Bearing Compound Fault Intelligent Diagnosis based on Vibration Signals

MIYAZAKI SHUUJI[1], ZHI-QIANG LIAO[2,3*], PENG CHEN[2*]
[1]Mitsubishi Chemical Corporation,
Okayama Prefecture Kurashiki city,
JAPAN

[2]Graduate School of Bioresources,
Mie University, Mie,
JAPAN

[3]Naval Architecture and Shipping College,
Guangdong Ocean University,
Zhanjiang,
CHINA

*Corresponding Authors

Abstract: - As a compound fault of bearing is characterized by complexity, disproportion, and interaction, its fault diagnostic accuracy tends to decline sharply. To solve this problem, the present study proposes a transient fault-signal extraction scheme for bearing compound fault intelligent diagnosis. First, the single fault vibration and compound fault vibration signals are transformed into the time-frequency domain by wavelet transform. Then, according to the normal condition signal, the transient fault signal of the single signal and compound signal is extracted through the positive k sigma principle. Next, the single fault signal symptom parameters are calculated to build the fault diagnostic model. Thereafter, the symptom parameters of the extracted compound fault transient signal are brought into the diagnostic model to obtain the model output result. Finally, according to the developed fault diagnosis discrimination criterion, the method can diagnose the compound fault successfully. The effectiveness of the proposed method is validated by bearing fault vibration signals under various conditions. The results show that the diagnostic method has superior performance in intelligently diagnosing the bearing compound fault.

Key-Words: - Compound fault, Fault signal extraction, Wavelet transform, Positive k sigma principle.

1 Introduction

Bearings are among the essential components of rotating machines. Due to their complex working conditions, bearing fault diagnosis is a significant task in guaranteeing equipment safety and reducing accidents, [1]. In many situations, compound faults often appear as spalls or cracks on different positions, [2]. Compared with fault diagnosis methods that have been successfully used in single faults, accurate diagnosis of compound faults has not been effectively proven in theory. Bearing compound fault is characterized by complexity, disproportion, and interaction results in diagnostic performance deterioration. Therefore, studying the compound fault diagnosis is important.

Many studies have conducted compound fault diagnosis of the rotating machine. With the development of automation and information technology, most methods are machine learning algorithms. The bearing compound fault diagnosis can be divided into two types: one is fault characteristic frequency-based and the other is discriminant model-based. The general process of the fault characteristic frequency-based type is as follows: the acquired signal is filtered first, and then a signal is decomposed to extract or strengthen the fault signal.

The method can identify the fault characteristic frequency for fault diagnosis. Numerous compound fault diagnosis strategies have been applied with this method, [3], [4]. Empirical mode decomposition,

[5], [6], empirical wavelet transform combined with chaotic oscillator, [7], 1.5-dimension envelope spectrum, [8], resonance and spectral kurtosis, [9], [10], Hilbert transform demodulation analysis, [11], and adaptive maximum correlated kurtosis deconvolution, [12], have been successfully applied with fault characteristic frequency-based approach. This type of method needs to calculate the fault characteristic frequency initially, which requires knowing intrinsic information about the object, such as size, rotation speed, and diameter. These factors are difficult to identify in some unknown working conditions. The general process of the discriminant model-based method is as follows: collecting the vibration signal in the fault state, extracting the fault features, and building an effective discriminant model for fault diagnosis through signal filtering and feature extraction. Many different studies have addressed compound fault diagnosis by this method. Sparse non-negative matrix factorization combined with support vector data description, [13], support vector machine, [14], [15], [16], independent component analysis, [17], principal component analysis, [18], [19], and hidden Markov model, [20], have been successfully applied in compound fault diagnosis. In this method, the accuracy of the discriminant model largely depends on the effective extraction of features, but no perfect method can be used to extract features in the compound fault signal characterized by feature coupling. Motivated by this problem, the present study developed an automatic transient spectrum extraction scheme for bearing compound fault diagnosis. Transient spectrum extraction can effectively extract single and composite fault features from signals, and the extracted features have stronger fault representation ability. Based on the transient spectrum extraction, the compound fault diagnosis model has better diagnostic ability.

The main contributions of this paper reflect in: (1) The proposed positive k sigma principle can extract single fault information from compound signals effectively. (2) The discriminant model with extracted single faults can reduce diagnostic performance deterioration caused by compound faults. Various experiments confirmed the efficacy of this method.

The rest of this paper is organized as follows. Section 2 introduces the bearing compound fault diagnosis method and theory proposed in this paper, which illustrates the positive k sigma principle to extract transient spectra and discrimination criteria. Section 3 uses the experiment platform data to verify the proposed method. Section 4 provides a summary of the conclusions.

2 Bearing Compound Fault Diagnosis Strategy

The automatic transient spectra scheme of bearing compound fault diagnosis covers condition surveillance, the positive k sigma principle, the discrimination model, and others. The process of the proposed method is shown in Figure 1.
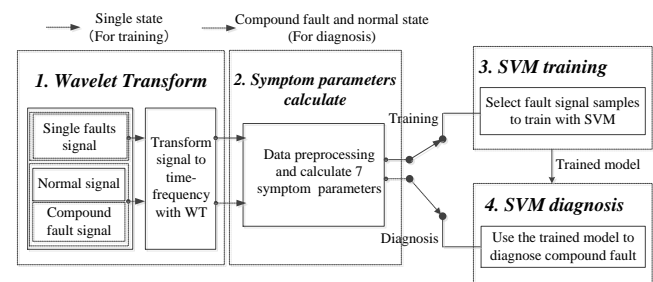

Fig. 1: Process of proposed compound fault diagnosis method

In the training stage, wavelet transforms (WT) are used to transform vibration signals measured in the normal state and single fault state (inner race, outer race, and roller defects) to the time-frequency domain. With normal state signals as reference signals, the transient spectra of abnormal (fault) states are detected. Each impulse wave corresponds to one transient spectrum. Then, the frequency domain symptom parameter method is used to obtain symptom values. These symptom values are synthesized as input and substituted into the support vector machine (SVM) to establish a model from symptom parameters to fault types.

In the diagnosis stage, condition surveillance is performed by measuring vibration signals to reveal the bearing condition first. Similar to the training stage, the compound fault is transformed into the time-frequency domain by WT. Then, the transient spectra of abnormal components are extracted using reference signals and the positive k sigma principle. In these transient spectra, frequency domain symptom parameters are used to obtain symptom values. Then, the symptom values are substituted into the SVM model, which is established in the training stage. According to the model result, the compound fault can be diagnosed through a designed discrimination criterion.

2.1 Condition Surveillance
The proposed bearing diagnosis method has two stages: one is condition surveillance (simple diagnosis) and the other is precision diagnosis. Before the diagnosis of compound faults, condition surveillance is needed to judge the bearing condition. Generally, for condition surveillance,

statistical symptom parameters acquired from vibration signals are used to monitor the mechanical condition. These parameters have two types: symptom parameters with dimensionality (e.g., mean and peak values representing signal amplitude) and dimensionless symptom parameters (e.g., skewness and waveform kurtosis, which represent signal shape), [21].

In the first step of the proposed method, the bearing condition must be diagnosed as either normal or not. Kurtosis is one of the most effective parameters to detect bearing abnormality. Kurtosis, which has been successfully used to detect bearing faults [22], is defined as

$$Kurtosis = \sum_{i=1}^{N}(x_i - \mu)^4 \bigg/ N\sigma^4 \qquad (1)$$

where: μ = mean value
σ = standard deviation
N = length of signal x_i

According to the experimental findings of reference, [22], when the bearing vibration signal kurtosis value exceeds five times the normal state signal kurtosis, the bearing is abnormal. Thus, kurtosis is employed for condition surveillance. It only judges whether the bearing is normal or not, and the further precise diagnosis employs the proposed method.

2.2 Discrete Wavelet Transform

Compared with the fast Fourier transform, wavelet transform, [23], [24] has good time-frequency localization properties in signal processing and characteristic of multi-resolution analysis. Given a signal $f(t)$, its discrete wavelet transform is defined as

$$DWT(j, k_{wt}) = \frac{1}{\sqrt{2^j}} \int_{-\infty}^{+\infty} f(t)\psi\left(\frac{t - 2^j k_{wt}}{2^j}\right) d(t) \qquad (2)$$

where: $\psi(t)$ = mother wavelet
2^j = scale parameter (inverse of frequency)
$2^j k_{wt}$ = translation parameter

2.3 Positive k Sigma Principle Fault-Transient Spectra Extraction Methodology

Using Eq. (2), i.e., wavelet transform computation, we can obtain time-frequency domain signals of each state for the training and diagnosis stages. Figure 2 shows the roller bearing vibration signal time domain fault impulse waveform of the abnormal state (Figure 2(a)) and the corresponding impulse waveform frequency spectrum transformed by WT in the time-frequency domain (Figure 2(b)).
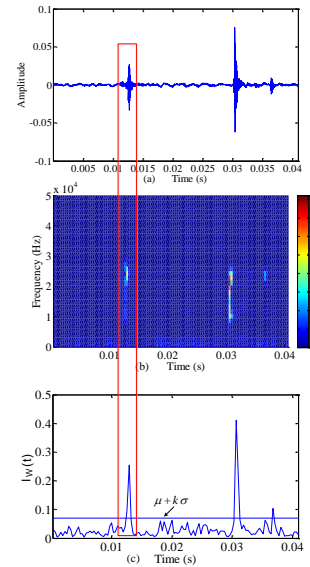

Fig. 2: Signals in time and time-frequency domains: (a) vibration signal; (b) time-frequency; and (c) time intensity of spectrum

To extract the transient spectra of the abnormal bearing, we define time intensity $I_w(t)$ of wavelet frequency spectrum $W(t_k, f_i)$ as follows:

$$I_W(t) = \sum_j \sum_{k_{wt}} \frac{1}{\sqrt{2^j}} f(t)\psi\left(\frac{t - 2^j k_{wt}}{2^j}\right) \qquad (3)$$

An example of $I_w(t)$ is presented in Figure 2(c). The value of $\mu + k\sigma$ exceeding reference state (normal state) $I_w(t)$ is normally used in selection to extract the transient spectra of fault pulse from the signals. Here, μ is the mean value of $I_w(t)$, σ is the standard deviation of $I_w(t)$, and k is calculated by

$$k = \left(\sum_{i=1}^{N_{peaks}} \left(I_{W_{peaks}}\right)_i \bigg/ N_{peaks}\right) \bigg/ \mu \qquad (4)$$

where: N_{peaks} = the number of peaks in the reference state (normal state)

2.4 Frequency-domain Symptom Parameters

To reflect symptoms of the fault-pulse signal transient spectrum as shown in Figure 2(c), according to our previous study, [21], seven types of frequency domain symptom parameters presented in Eqs. (5–11) are used to represent symptoms of the transient spectrum.

$$p_1 = \sqrt{\sum_{i=N/3}^{N} f_i^2 S(f_i) \bigg/ \sum_{i=N/3}^{N} S(f_i)} \qquad (5)$$

$$p_2 = \sqrt{\sum_{i=N/3}^{N} f_i^4 S(f_i) \bigg/ \sum_{i=N/3}^{N} f_i^2 S(f_i)} \qquad (6)$$

$$p_3 = \sum_{i=N/3}^{N} f_i^2 S(f_i) \bigg/ \sqrt{\sum_{i=N/3}^{N} f_i^2 S(f_i) \sum_{i=N/3}^{N} S(f_i)} \qquad (7)$$

$$p_4 = \frac{\sigma}{\bar{f}} \qquad (8)$$

$$p_5 = \sum_{i=N/3}^{N} \left(f - \bar{f}\right)^3 S(f_i) \bigg/ \sigma^3 N \qquad (9)$$

$$p_6 = \sum_{i=N/3}^{N} \left(f - \bar{f}\right)^4 S(f_i) \bigg/ \sigma^4 N \qquad (10)$$

$$p_7 = \sum_{i=N/3}^{N} \sqrt{\left|\left(f - \bar{f}\right)\right|} S(f_i) \bigg/ \sqrt{\sigma} N \qquad (11)$$

here,

$$\bar{f} = \sum_{i=N/3}^{N} f_i S(f_i) \bigg/ \sum_{i=N/3}^{N} S(f_i)$$

$$\sigma = \sqrt{\sum_{i=N/3}^{N} \left(f - \bar{f}\right)^2 S(f_i) \bigg/ N}$$

where: N = the acquired signal length

f = the frequency of the acquired signal

$s(f)$ = signal frequency spectrum, $i = 1, 2, \cdots N$.

The amplitude $s(f)$ significantly influences the value of such a symptom parameter. Before the symptom parameters are calculated, both the spectrum and symptom parameters should be normalized.

$$s(f) = s'(f) \bigg/ \sum_{f=1}^{N/2} s'(f) \qquad (12)$$

where: $s(f)$ = the spectrum of normalization

$$p_i' = (p_i - \bar{p}) \big/ std_{p_i} \qquad (13)$$

where: p_i: fault symptom parameter;

p_i': fault symptom parameter of normalization;

$\bar{p}$: the mean value symptom parameter;

std_{p_i}: the standard deviation symptom parameter.

2.5 Classification of Compound Faults by SVM

SVM is a type of intelligent algorithm based on the theory of statistical learning. As bearings have many fault types, compound fault SVM is a multi-class classification problem.

Based on the normal state of bearing, according to Eqs. (5–11), single-fault symptom parameters are

P_{jk_i} ($j = 1–M$, $k_i = O, I, R$), $k = O$ (outer race defect), I (inner race defect), and R (roller defect). Their instantaneous spectra and symptom parameters are normalized. Seven symptom values are input parameters to SVM and the fault type is the output.

After training the SVM model, compound fault parameters P_{jc} ($j = 1–M$), where C indicates compound faults, are substituted into the model to identify the fault type.

2.6 Discrimination Criterion

Based on the SVM classification model, the model output is used to identify the compound fault type. This study proposes a discrimination method based on cumulative percentage, which is defined as follows:

We assume that N_x, $x = 1,2,\ldots,m$ is the number of fault type output by SVM and m is the fault type. N_x is ranked as $N_1 \geq N_2 \ldots \geq N_m \geq 0$ individual percentage, and pr_i is defined as

$$pr_i = N_i \bigg/ \sum_{i=1}^{m} N_i \qquad (14)$$

The cumulative percentage of the first t type in the sequence is defined as

$$C_t = \sum_{i=1}^{t} N_i \bigg/ \sum_{i=1}^{m} N_i, \quad t = 1,2,\cdots m \qquad (15)$$

As compound faults are characterized by multiplicity and coupling, some fault symptoms are not sufficiently clear. The proposed method is implemented to assess the number of single faults in the compound faults. However, the existence of noise, complex fault signals, and coupling features lead to a condition in which the single fault cannot be perfectly (100%) extracted from the compound fault signal. Thus, dominant signals of single faults are selected to diagnose compound faults. The threshold Thr is provided to select t. If $C_t \geq Thr$, then the compound faults include the first t fault types. Here, the threshold Thr refers to principal component analysis theory: the percentage of the cumulative sum over 80% can represent the main information of the signal. Fault discrimination operations are shown in the following steps:

Step 1: The diagnosis samples are brought into the trained model of SVM and obtain the classification result N_i.

Step 2: All N_i values are ranked from max to min $N_1 > N_2 \cdots > N_m$.

Step 3: Cumulative percentage $Pr_i = \sum_{i=1}^{t} N_i \bigg/ \sum_{i=1}^{m} N_i$, where $Pr_i, i = 1,2,\cdots m$ is calculated.

Step 4: Fault type is diagnosed; if $Pr_i \geq Th_r$, then a fault type exists from 1 to i.

For example, given the SVM model fault type output ranking of $N_o > N_I > N_R$, if $(N_o+N_I)/(N_o+N_I+N_R) \geq Thr$, the compound fault includes O (outer race defect) and I (inner race defect). If $(N_o)/(N_o+N_I+N_R) \geq Thr$, then only the outer race defect O exists.

3 Experiment

3.1 Experimental Conditions

To verify the effectiveness and feasibility of the proposed method, this study presents the results of roller-bearing compound fault diagnosis tests performed on a rotating experimental machine facility (Figure 3). An experimental bench used for fault diagnosis testing is provided and includes loading equipment, a servo motor, and a rotor system. The original vibration signals of each state were measured by an accelerometer with a sampling frequency of 100,000 Hz. Objects of diagnosis include a single fault in Figure 4 (outer race defect, inner race defect, and roller defect) and a compound fault (inner race defect and outer race defect, inner race defect and roller defect, and outer race defect and roller defect) created by machining. The inner race defect is 0.15 mm × 0.5 mm (depth × width), the outer race defect is 0.15 mm × 0.5 mm (depth × width), and the roller defect is 0.15 mm × 0.5 mm (depth × width). The accelerometer is installed in the vertical direction of the bearing seat (1,500 revolutions per minute). The length of the experiment data is 16,384.
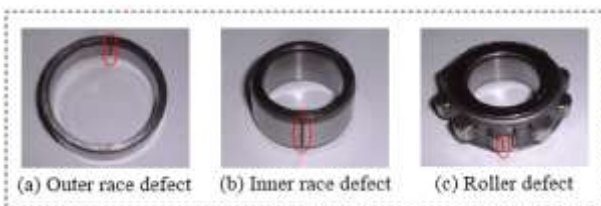

Fig. 3: Experimental bench

Fig. 4: Fault bearing for test: (a) outer race defect, (b) inner race defect, and (c) roller defect

This experiment adopts a compound fault that includes inner race and roller defects as an object to verify the effectiveness of the proposed method. If the fault-state operating conditions of the bearing experiment differ from the normal state, then the diagnostic accuracy declines.

3.2 Condition Surveillance

Kurtosis analysis is used for condition surveillance. According to theory, in the normal state, the kurtosis value is near 3 and the probability distribution follows the normal distribution. If the kurtosis value exceeds 5 times the normal state, then faults exist in the bearing. The farther the kurtosis value from 5, the more serious the fault. This study adopts vibration signals of the normal state, single fault, and compound fault to calculate the time domain kurtosis values. Results are provided in Table 1.

Table 1. Kurtosis Values of Each State

Type	Kurtosis Value
Normal state	2.869
Inner race defect state	109.2879
Outer race defect state	34.1227
Roller race fault state	253.4692
Compound fault state	74.84

As shown in Table 1, the normal state kurtosis value is near 3. The kurtosis values of the inner race defect, outer race defect, roller defect, and compound fault are 109.2879, 34.1227, 253.4692, and 74.84, respectively. All of these values are larger than 5 times the normal state. This result indicates the fault in measured vibration signals. To allow a straightforward analysis, Figure 5 shows the calculated probability density distribution of each state.
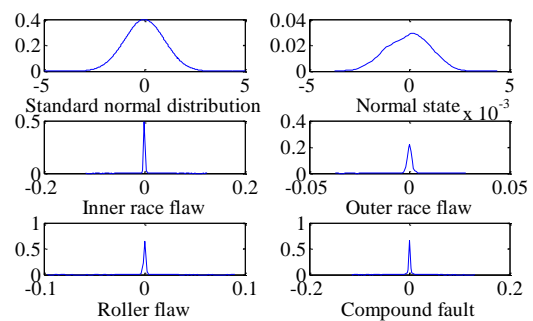

Fig. 5: Probability distribution of each state

As presented in Figure 5, according to the standard normal distribution, the probability

distribution of the normal state follows the normal distribution. The probability distributions of the inner race, outer race, and roller defects deviate from the normal distribution. The more apparent this deviation, the more apparent the fault. Compared with the normal distribution, the compound fault kurtosis value deviates from the normal distribution.

3.3 Extraction of Transient Spectra using WT

Considering the characteristics of vibration signals, this study adopts Gabor wavelet $\psi(t)$ to transform signals to the time–frequency domain.

$$\psi(t)=g_\sigma(t)e^{it} \qquad (16)$$

where: $g_\sigma(t)$ is referred to as the Gaussian window function defined as

$$g_\sigma(t)=\frac{1}{\sqrt{2\pi}\sigma}e^{-\frac{(t-\mu)^2}{4\sigma^2}} \qquad (17)$$

where: σ = the standard deviation (factor width)
μ = the mean value (time factor)

Through WT operations, time–frequency diagrams of a normal state, single fault state, and compound fault state are obtained. The example of the inner race defect result is shown in Figure 6.

In Figure 6, (a) shows vibration signals acquired by the experiment, (b) shows some data of the time domain signals intercepted from (a), (c) shows the time–frequency contour diagram of the wavelet spectrum obtained by WT, and (d) shows the time intensity of the wavelet spectrum. As presented in Figure 6, the fault pulse in the vibration signal time domain has a corresponding fault symptom transient spectrum in the time–frequency domain. The time-intensity of $I_w(t)$ of this point exceeds the time intensity when no pulse signal exists. With the normal state as a reference, the positive k sigma principle $\mu+k\sigma$ of $I_w(t)$ is used as the method to select fault-signal transient spectra. According to experiment results, $\mu+6\sigma$ has been used to extract 88 transient spectra from a single inner-race defect, $\mu+4\sigma$ has been used to extract 118 transient spectra from a single outer-race defect, $\mu+3\sigma$ has been used to extract 104 transient spectra from a single roller defect, and $\mu+3\sigma$ has been used to extract 153 transient spectra from a compound fault.

Obtained transient spectra have been normalized and then, symptom parameters in Eqs. (5–11) are used to obtain symptom values of the transient spectra, followed by normalizing of symptom parameters using Eqs. (12–13).

After the operations mentioned, the data obtained can be used to establish the classification model and identify and diagnose the compound faults.
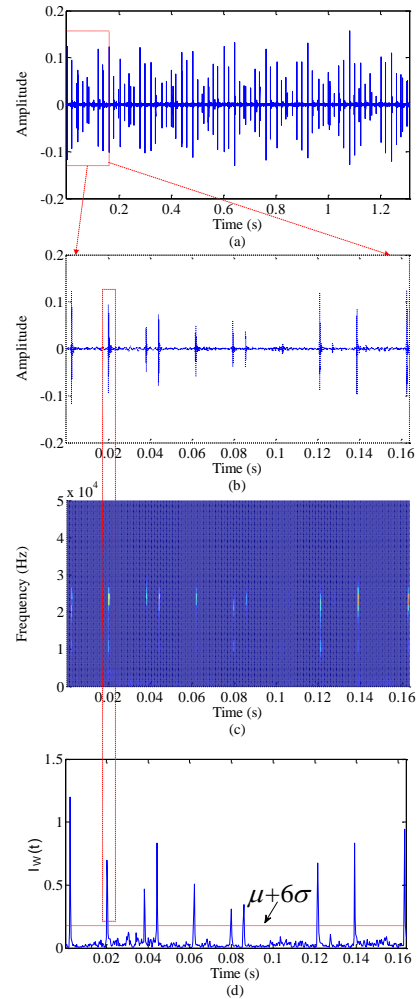

Fig. 6: Fault signal time domain and time–frequency domain (inner race defect)

3.4 Diagnosis of Compound Faults

In this section, SVM is used to establish a roller-bearing diagnosis model. Based on this built model, the compound fault can be classified. Some symptom parameters of the SVM model training part are inner race defect: 1(type), outer race defect: 2(type), and roller defect: 3(type). Diagnosis parts (compound faults) are presented in Table 2.

Table 2. Diagnosis samples

State	Fault type	No.	P_1	…	P_7	Fault type
Training	Inner	1	0.802	…	2.373	1
		…	…	…	…	1
		60	0.048	…	3.338	1
	Outer	61	1.212	…	2.912	2
		…	…	…	…	2
		120	0.864	…	2.684	2
	Roller	123	0.877	…	3.936	3
		…	…	…	…	3
		180	1.098	…	3.163	3
Diagnosis	Compound	181	2.47	…	0.774	Unknown
		…	…	…	…	Unknown
		333	0.343	…	2.86	Unknown

Here, the SVM model uses RBF as the kernel function. In the training stage, 60 symptom parameter samples of each state of the inner race defect, outer race defect, and roller defect (total of 180 samples) are taken to train the SVM model. Additionally, 24 symptom parameter samples of each state are taken as test samples to test the model. After the model training, the 153 symptom parameters calculated from the compound fault state are used as diagnosis samples to diagnose the compound fault, as shown in Table 3.

Table 3. Sample setting of the SVM model

	Fault type	Training samples	Test samples
Training state	Inner	60	24
	Outer	60	24
	Roller	60	24
Diagnosis state	Compound	No	153 (for diagnosis)

All single-fault (inner race, outer race, and roller defects) training samples are used to train the SVM model. Then, testing samples of all single faults are used to test the trained model. The model test accuracy is defined as:

$$Accuracy = \frac{\sum correctSamples}{\sum testingSamples}\% \qquad (18)$$

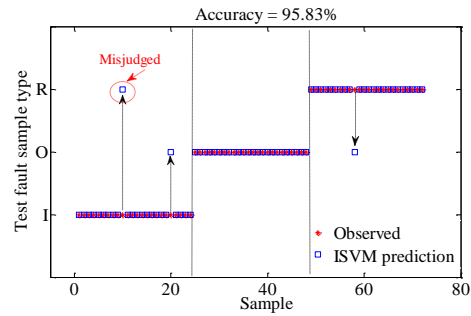The model test results are presented in Figure 7.

Fig. 7: Accuracy of a test sample of the SVM model (*I*: inner, *O*: outer, and *R*: roller)

As shown in the results, output result accuracy reaches 95.83%, thereby indicating the good performance of the training model and the successful establishment of mapping from fault symptom parameters to fault types. Based on this trained model, symptom parameters of compound fault are substituted into the model to verify the type of compound fault.

Substituting the 153 calculated compound fault symptom parameters into the built SVM model, we find that the output of the model belongs to three types (*I*: inner race defect, *O*: outer race defect, and *R*: roller defect). According to Eq. (14), N_I is 38 and its percentage P_I is 24.84%; N_O is 19 and its percentage P_O is 12.42%, and N_R is 96 and its percentage P_R is 62.74%. Based on the ranking of a percentage from maximum to minimum, and using Eq. (15), the cumulative percentage of each fault state (C_I, C_O, and C_R) has been calculated, with results shown in Figure 8.
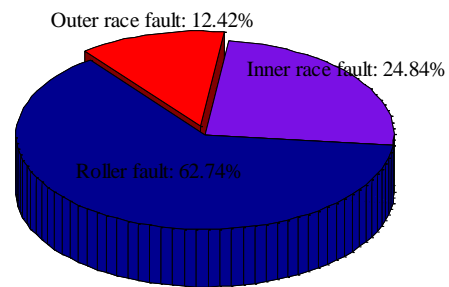

Fig. 8: Fault type in compound fault

According to the results, the fault types are ranked as follows: roller, inner race, and outer race defects. As the data in the table show, the cumulative percentage of the second (fault types: roller defect and inner race defect) is 87.58%, which indicates the inner race and roller defects in the compound fault. This result is consistent with the experimental facility, indicating the effectiveness of the proposed method.

To further prove the effectiveness of this method, we have tested three types of single fault (inner race, outer race, and roller defects) and another type of compound fault (outer race defect + roller defect). Verification results are presented in Table 4.

As shown in Table 4, if the diagnostic proportion of a certain type of fault in the signal exceeds 95%, it indicates that there is only one type of fault. For composite faults, according to the method mentioned in Section 2.6, the cumulative percentage of extracted faults is 89.54%, exceeding 80%, indicating that it is a compound fault and proving that the diagnosis is effective.

Table 4. SVM fault diagnosis in single fault and compound faults

No.	Classifica-tion of fault	Classified correctly	Misjudged datasets	Accur-acy (%)
1	I	N_I:21 (I)	1 (others)	C_I: 95.23
2	O	N_o:24 (O)	0	C_o: 100
3	R	N_R: 22 (R)	1 (others)	C_R: 95.45
4	O and R	N_{R+O}: 124 (O and R)	13 (others)	C_{R+O}: 89.54

(I: inner race defect, O: outer race defect, R: roller defect.)

3.5 Diagnosis of Compound Faults

To further prove the effectiveness and advancement of this proposed method, we employed the conventional method for comparison with the developed method. The main steps of the conventional method are the following: (1) dividing the compound fault vibration signal by N signal subsets, (2) every signal subset attracts frequency domain symptom parameters according to Eqs. (5–11), (3) the symptom parameters are placed in the SVM model by single fault symptom parameters, and (4) the discrimination criterion is used to calculate the diagnosis accuracy. The results are shown in Table 5.

The results in Table 5 show that the conventional method was used in single-fault diagnosis, and the diagnosis accuracy approximates the proposed method. When the conventional method was used in the compound fault of the roller bearing, the

conventional method had a low accuracy (the cumulative percentage of the outer race defect and roller defect is 56.45%). These results show that the proposed method can reduce the diagnostic performance deterioration caused by compound faults in roller bearing diagnosis.

Table 5. Results of proposed and conventional methods

No.	Classifica-tion of fault	Classified correctly	Proposed method accuracy (%)	Conven-tional method accuracy (%)
1	I	N_I: 21 (I)	C_I: 95.23	C_I: 95.23
2	O	N_o: 24 (O)	C_o: 100	C_o: 95.85
3	R	N_R: 22 (R)	C_R: 95.45	C_R: 95.45
4	O and R	N_{R+O}: 124 (O and R)	C_{R+O}: 89.54	C_{R+O}: 56.45

(I: inner race defect, O: outer race defect, R: roller defect.)

3.6 Different Fault Severity in Compound Faults

When the compound fault vibration signal has different fault-severity bearing components, the proposed method's efficacy depends on the fault degree. If the positive k sigma principle can extract the transient spectra of all the single faults, then different fault-severity bearing components can be diagnosed using the developed method. If the positive k sigma principle cannot extract certain transient spectra, then the slight fault (which was not extracted) can be regarded as a noise signal and does not affect the operation, and the compound fault cannot be effectively diagnosed.

The following experiments are conducted to verify our findings. Two compound fault roller-bearing vibration signals are observed: the first compound fault signal composed of inner race defect is 0.15 mm × 0.5 mm (depth × width) and the roller defect is 0.05 mm × 0.3 mm (depth × width). The roller defect severity is slight compared with the inner race defect. The second compound fault signal is composed of the outer race defect 0.15 mm × 0.3 mm (depth × width) and roller defect 0.15 mm

× 0.5 mm (depth × width). The results of the positive *k*-sigma principle of the developed method are shown in Figure 9.
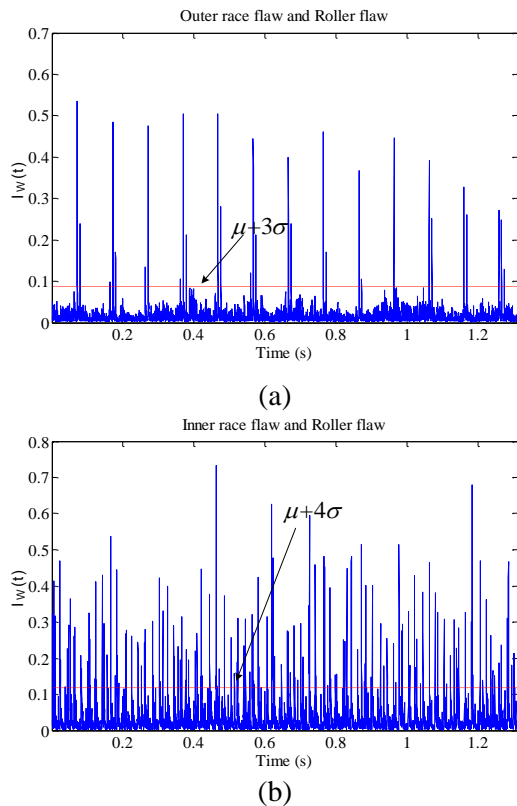

(a)

(b)

Fig. 9: Different fault-severity diagnosis results:
(a) compound fault: outer race and roller defects;
(b) compound fault: inner race and roller defects

After the operation by the SVM model, in the compound fault, the percentage of the outer race defect is 86.36%. If larger than 80%, then the roller defect cannot be accurately diagnosed. The reason is that the roller defect degree is slight and cannot extract the single fault (roller defect) feature by the positive *k* sigma principle. In the compound fault, the cumulative percentages of the inner race and roller defects are 92.91% (roller defect: 49.61% and inner race defect: 43.31%). The compound fault diagnosis result is correct. Therefore, when the severity of a single fault in a composite fault signal is different, the positive *k* sigma principle can extract the transient spectrum of a single fault as a feature. If the transient spectrum cannot be extracted, it is considered a noise signal.

4 Conclusion

An automatic transient-spectra extraction scheme was developed to reduce diagnostic performance deterioration caused by compound faults in roller bearing diagnosis. The single fault features were extracted from the compound fault vibration signal by a positive *k* sigma principle. The created diagnosis discrimination criterion is the ratio of the single components to the multiple components estimated by understanding the relationship between the single and compound faults. The developed method was verified through various conditions of the defective roller bearing by the SVM model. The experimental results indicated that the developed method was superior to the conventional method in compound fault diagnosis.

In the future, this method can be applied to other rotating machines, such as in the diagnosis of gear faults. At the same time, the complexity and time consumption of the developed method have to be considered in future research.

References:
[1] Zhang, X.j., Jirui Z., Wu Y.Q., Dong Z., Zhang M.L., Feature Extraction for Bearing Fault Detection Using Wavelet Packet Energy and Fast Kurtogram Analysis, *Applied Sciences*, Vol.10, No.21, 2020, pp. 7715.

[2] Zheng, K., Jia, G.Z., Yang L.C., Wang J.Q., A Compound Fault Labeling and Diagnosis Method Based on Flight Data and Bit Record of Uav, *Applied Sciences*, Vol.11, No.12, 2021, pp. 5410.

[3] Zhang, J.F., Zhang Q.H., He X., Sun G.X.& Zhou D.H., (2021). "Compound-Fault Diagnosis of Rotating Machinery: A Fused Imbalance Learning Method." *IEEE Transactions on Control Systems Technology*, Vol.29, No.4, 2021, pp. 1462-1474.

[4] Jing, M., Wang, H., Zhao, L.Y., Yan R.Q., Compound Fault Diagnosis of Rolling Bearing Using Pwk-Sparse Denoising and Periodicity Filtering, *Measurement*, Vol.181, No.107736, 2021, pp. 109604.

[5] Li, Z.X., Jiang, Y., Hu, C.Q., Peng, Z.X., Difference equation based empirical mode decomposition with application to separation enhancement of multi-fault vibration signals, *Journal of difference equations and applications*, Vol.23, 2017, pp. 457-467.

[6] Sun, Y.J., Li S.J., Wang X.H, Bearing Fault Diagnosis Based on EMD and Improved Chebyshev Distance in SDP Image,

Measurement, Vol.176, No.17, 2021, pp. 109100.

[7] Jiang, Y., Zhu, H., Li, Z., A new compound faults detection method for rolling bearings based on empirical wavelet transform and chaotic oscillator, *Chaos, Solitons & Fractals*, Vol.89, 2016, pp. 8-19.

[8] Yan, X.A., Jia, M.P., Xiang, L., Compound fault diagnosis of rotating machinery based on OVMD and a 1.5-dimension envelope spectrum, *Measurement Science and Technology*, Vol.27, No.17, 2016, pp. 075002.

[9] Wang, T.Y., Chu, F.L., Han, Q.K., Kong, Y., Compound faults detection in gearbox via meshing resonance and spectral kurtosis methods, *Journal of Sound and Vibration*, Vol.392, 2017, pp. 367-381.

[10] Zhang, X., Wan S.T., He Y.L., Wang X.L., Dou L.J., Teager Energy Spectral Kurtosis of Wavelet Packet Transform and Its Application in Locating the Sound Source of Fault Bearing of Belt Conveyor, *Measurement*, Vol.173, 2021, pp. 108367.

[11] Chen, J.L., Zi, Y.Y., He, Z.J., Yuan, J., Compound faults detection of rotating machinery using improved adaptive redundant lifting multiwavelet, *Mechanical Systems and Signal Processing*, Vol.38, No.4, 2013, pp. 36-54.

[12] Tang, G.J., Wang, X.L., He, Y.L., Diagnosis of compound faults of rolling bearings through adaptive maximum correlated kurtosis deconvolution, *Journal of Mechanical Science and Technology*, Vol.30, No.1, 2016, pp. 43-54.

[13] Wang, H.C., Fault diagnosis of rolling element bearing compound faults based on sparse no-negative matrix factor-ization-support vector data description, *Journal of Vibration and Control*, Vol.24, 2018, pp. 272-282.

[14] Bensaoucha, S., Youcef B., Sandrine M., Sid A. B., Aissa A., Induction Machine Stator Short-Circuit Fault Detection Using Support Vector Machine, *Compel-the International Journal for Computation and Mathematics in Electrical and Electronic Engineering*, Vol.2021, No.3, 2021, pp. 40.

[15] Chen, F.F., Tang, B.P., Song, T., Li, L., Multi-fault diagnosis study on roller bearing based on multi-kernel support vector machine with chaotic particle swarm optimization, *Measurement*, Vol.47, 2014, pp. 576-590.

[16] Liu, Z., Cao, H., Chen, X., He, Z., Shen, Z., Multi-fault classification based on wavelet

SVM with PSO algorithm to analyze vibration signals from rolling element bearings, *Neurocomputing*, Vol.99, 2013, pp. 399-410.

[17] Li, Z.X., Yan, X.P., Tian, Z., Yuan, C.Q., Peng, Z.X., Li, L., Blind vibration component separation and nonlinear feature extraction applied to the nonstationary vibration signals for the gearbox multi-fault diagnosis, *Measurement*, Vol.46, No.4, 2013, pp. 259-271.

[18] Yan, R.Q., Shen F., Zhou M.J., Induction Motor Fault Diagnosis Based on Transfer Principal Component Analysis, *Chinese Journal of Electronics*, Vol.30, No.1, 2020, pp. 18-25.

[19] Hwang, S.Y., Kim K.S., Kim H.J., Jun H.B., Lee J.H., Application of Pca and Classification for Fault Diagnosis of Mab Installed in Petrochemical Plant Process Facilities." *Applied Sciences*, Vol.11, No.9, 2021, pp. 11093780.

[20] Purushotham, V., Narayanan, S., Prasad, S.A.N., Multi-fault diagnosis of rolling bearing elements using wavelet analysis and hidden Markov model based fault recognition, *NDT & E International*, Vol.38, No.8, 2005, pp. 654-664.

[21] Wang, H., Chen, P., Intelligent Methods for Condition Diagnosis of Plant Machinery, *InTech*, 2011, pp. 119-140.

[22] Antoni, J., Randall, R., The spectral kurtosis: application to the vibratory surveillance and diagnostics of rotating machines, *Mechanical Systems and Signal Processing*, Vol.20, 2006, pp. 308-331.

[23] Chen, J., Li, Z., Pan, J., Chen, G., Zi, Y., Yuan, J., Chen, B., He, Z., Wavelet transform based on inner product in fault diagnosis of rotating machinery: A review, *Mechanical Systems and Signal Processing*, Vol. 70–71, 2016, pp. 1-35.

[24] Qin, C., Wang G.D., Xu Z., Tang G., Improved Empirical Wavelet Transform for Compound Weak Bearing Fault Diagnosis with Acoustic Signals, *Applied Sciences*, Vol.10, No.2, 2020, pp. 10020682.

Contribution of Individual Authors to the Creation of a Scientific Article (Ghostwriting Policy)
The authors equally contributed to the present research, at all stages from the formulation of the problem to the final findings and solution.

Conflict of Interest
The authors have no conflict of interest to declare.